



PADC-NTM Applied in ${}^7\text{Li}+\text{Pb}$ at 31 MeV Reaction Products Study

M. Cinausero¹, A. M. Sajo-Castelli², L. Sajo-Bohus², J. Palfalvi³ and G. Espinosa^{4*}

¹National Laboratories of Legnaro, I-35020 Legnaro (Pd), Italy

²Nuclear Physics Laboratory, Simón Bolívar University, Caracas 1080A, Venezuela

³HAS KFKI Atomic Energy Research Institute POB 49, H-1525 Budapest, Hungary

⁴Institute of Physics, National Autonomous University of Mexico, Coyoacán, México City

*Email: espinosa@fisica.unam.mx

ARTICLE INFORMATION

Received: October 10, 2019

Accepted: January 21, 2020

Published online: February 28, 2020

Keywords:

Nuclear tracks, PADC, ${}^7\text{Li}+\text{Pb}$ reaction products identification, 8pLP, Track spectrum unfolding



DOI: [10.15415/jnp.2020.72013](https://doi.org/10.15415/jnp.2020.72013)

ABSTRACT

Passive nuclear track methodology (NTM) is applied to study charged particles products of the reaction ${}^7\text{Li}+\text{Pb}$ at ~ 31 MeV. It is a contribution to the 8pLP Project (LNL-INFN-Italy) in where we show an alternative approach to register charged particle from reaction fragments by PADC detection. The main advantage is that the passive system integrates data over the whole experiment and has its importance for low rate reaction processes. Reaction products as well as scattered beam particles are determined from track shape analysis. Some limitations are inherent to NTM since a priori knowledge is required to correlate track size distribution given by each type of particle emerging from the target. Results show that the passive technique gives useful information when applied in reaction data interpretation for a relatively large range of particle types.

1. Introduction

Nuclear track detector methodology (NTM) is given for charged particle identification produced during nuclear reaction in experimental studies at LNL facility. The facility detecting system has 8pLP arrangements characterized by high flexibility, long path for time of flight (TOF) technique and geometry, being the latter a setup of two concentric active detector arrays. The apparatus detailed technical features are given by Fioretto et al. [1]; essentially is an assembly of a compact active type detector with $\sim 4\text{p}$ solid angle. The telescope type assembly is characterized by the large solid angle (90% of 4π) and its 262 modules of high granularity. Particle identification at low energy is enhanced by combining $\Delta E-E$, TOF and pulse shape discrimination (PSD) techniques. Thresholds for particle identification range from 1MeV for protons and 3MeV for alpha particles to about 2–3AMEV for C ions. These particles charge and energy, are in the PADC (Poly Allyl-Diglycol-Carbonate) detecting range; therefore ${}^7\text{Li}+\text{Pb}$ at 31 MeV reaction products cope with the requirements to test the response to complex and relatively low charge energy radiation. The data collection occurs in an integral form through latent track formed in the mentioned plastic detectors matter. In this study a 1 mm thick passive detector of a $\text{C}_{12}\text{H}_{18}\text{O}_7$

compound with a density of 1.30 g cm^{-3} was used and has the commercial trade name of TASTRAK (TASL Ltd, Bristol, UK); the company supplied the detectors for this study. These low-cost passive devices, detect efficiently protons above 500keV kinetic energy and heavier charged particles with energy greater than 200keV, making them particularly of advantage in nuclear reaction studies mainly when long term data integration is an issue. One of the difficulties in mixed particle beam identification or complex reaction products is often the lack of a precise correspondence between impinging particles charge mass and energy, and etched tracks. The reason is related to charged particle energy and mass induction of latent tracks; further interference is related to chemical etching to form track geometry pit diameter and detector sensitivity. High Z-value and energetic (HZE) particle in PADC detectors response has been studied by Palfalvi et al. [2] considering their exposure to mono energetic particles from a low intensity beam. Studies were made to interpret complex nuclear tracks [3,4]. However, development on the etched track-particle correspondence is still active, suggested employing successive etching time to improve the technique by demonstrating the necessity to include LET-value (Linear Energy Transfer) measurement to determine PADC-response. In spite of the shortcomings, passive detectors are applied with success for reaction

fragment studies; related information reported in the literature support the initiative to employ passive detectors to study ${}^7\text{Li}+\text{Pb}$ reaction products. NTM to identify low “Z” particles from a multivariate track offer several technical advantages compared to complex active detecting systems (that may have several dozens of costly Silicon Surface Barrier Detectors (SSBD)). The priory knowledge of some parametric value is necessary to determine the best particle-etched track correlation, for instance: track etch rate ratio ($V=VB/VT$), LET and removed layer thickness, Δh , during the chemical etching process. Values of these parameters depend on the chemical solution (composition, temperature and time for a given plastic batch) other than manufacturing process (such as curing PADC cycle). Keeping constant only the etching parameters (NaOH concentration, etching temperature and time) as much as possible, is not enough since it may lead to erroneous particle identification; the removed layer Δh should be obtained from the fitted equation:

$$\Delta h = 104.809 - 104.857 e^{-d/131.117} \quad (1)$$

where d is the mean diameter of the alpha tracks as given.

2. Experimental Set-Up

A PADC detector of size ($1 \times 2 \text{ cm}^2$) is positioned on the place left by removing one of the Si detectors and its supporting box, from its position labelled by “109” in the target “ball” chamber at 29 degrees relative to a telescope of the LNL Tandem XTU-ALPI superconducting LINAC facility (see Figure 1).

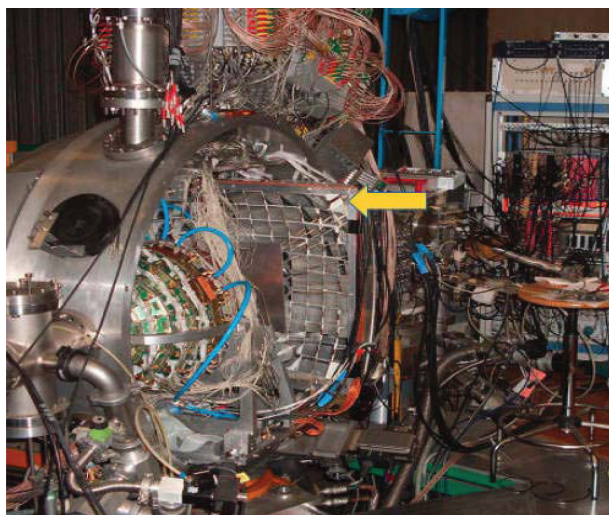


Figure 1: The 8pLP target “ball” chamber at the LNL Tandem XTU-ALPI superconducting LINAC facility. The arrow shows the PADC-CR39TM-detector at position “109”, relative to the telescope at 29 degrees.

The PADC is bolted onto a plastic frame, covering a smaller solid angle in comparison to the active detectors. The irradiations were carried out bombarding with a beam of ${}^6\text{Li}$ a $400 \mu\text{g}/\text{cm}^2$ self-supporting CD_2 target ($E_{\text{beam}}=31\text{MeV}$; $i_{\text{beam}}=10\text{nA}$). Detector (CR-39TM) is positioned at a forward angle of 29 degrees. It is expected to provide information through etched tracks, on light particles (p, d, t) and heavy ion such as (a, Li, C) originating from beam-target interactions. Reaction products impinging on the detector surface, penetrate few microns in the PADC matter leaving a latent track. The damaged and the undamaged matter, under chemical etching behave differently Dörschel [5] offering by *de facto* the possibility to discriminate between impacting particle energy and mass through geometry of etched tracks analysis employing digitalized images. In this study the MORFOLM track analyser program (developed at AEKI, Budapest, Hungary) is employed. Tracks appear on the detector surface as darker regions visible under optical transmission microscope. A 6N, NaOH aqueous solution at 70°C , is applied in a two-step sequence: first, etching is carried out for 2h and then depending on the observed tracks characteristics, it is etched for 2h more. The chemical processing is conveniently made in a thermostatic water bath with convection stirring. After the preset etching time, the detector is rinsed in distilled water in an ultrasonic cleaning unit. A semi-automatic track analyser provides information on track geometrical parameters such as area, perimeter, convexity, size and others related to collected beam-like particles and reaction fragments [6]. Track size is recorded in a histogram to which Gaussian fit deconvolution is applied for further data interpretation

2.1 Nuclear Track and Particle Identification

The charged particle energy deposition follows the typical Bragg curve, and along the absorption path length a high-density plasma induces a cylindrical damage with diameters in the range of 100 to 1000 nm which can be directly visualized without chemical etching. Direct observation of latent nuclear tracks in organic material can be visualized by atomic force microscopy [7]. However, these are conveniently enlarged taking advantage of the fact that track etching velocity ratio $V = (v_T/v_B)$ between the track v_T and bulk etching rate v_B is greater than one ($v_T > 5 v_B$). Lounis suggested that given the restricted energy loss (REL) the parameter V can be expressed as $V(\text{REL}350) = 0.3763 \text{ REL}$ 0.3142. The track diameter D (mm), under the assumption of constant v_T , can be determined from the following equation [8]:

$$\frac{v_T}{v_B} = 1 + \frac{L_e}{v_B t} = \frac{1 + (D/2v_B t)^2}{1 - (D/2v_B t)^2} \quad (2)$$

Combining the empirical expression of Lounis et al. and the velocity ratio V of equation 2, the track diameter assumes the following relation [8]

$$D(\mu m) = 2\nu_b t \left[\frac{[V(REL_{350}) - 1]}{[V(REL_{350}) + 1]} \right]^{0.5} \quad (3)$$

Track diameter for a large set of ions is therefore expressed by the bulk etching velocity and time (that for a given case is a constant) times a discriminating factor assumed to be constant as a first approximation for a given absorbed particle.

2.2 Etched track Analysis

The analyser software has incorporated a pattern recognition feature to segment the track; this procedure makes it particularly suitable for complex track analysis as Palfalvi et al., pointed out [2, 6, 9]. In Figure 2 shows etched tracks given by the MORFOLM code, at the left side of the screen a histogram bar recollects the data on track size distribution.

we obtained the following relationship between etching time (t_{etch}) and track radius: R_{track} (μm),

$$R_{track} = 0.7686(t_{etch})^{1.03} \quad (4)$$

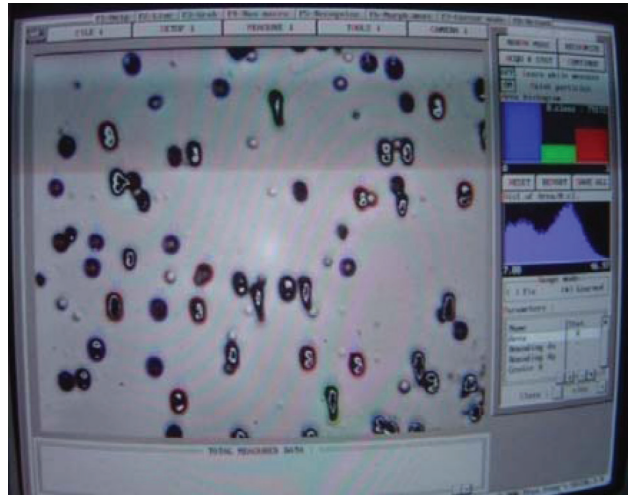


Figure 2: Displayed data of etched tracks as given by the MORFOLM code. At the right side on the screen shot, tracks size distribution histogram is shown and below it, a list of parameters through which tracks are analysed (macro processing sequence).

3. Results

From the data on etched tracks diameters of alpha particles (collimated polonium-210 source) given in Figure 3 (at left)

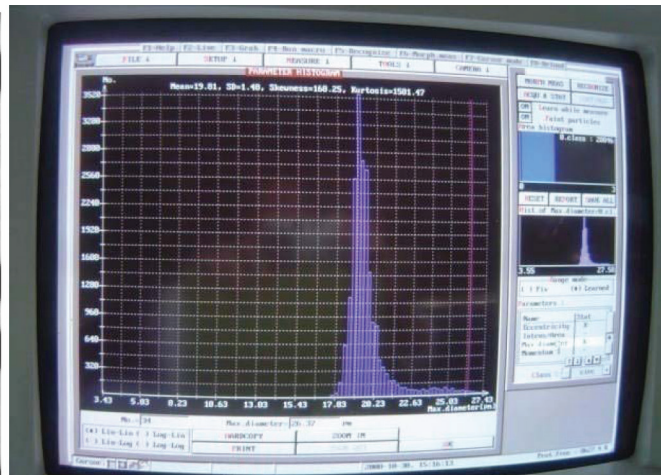
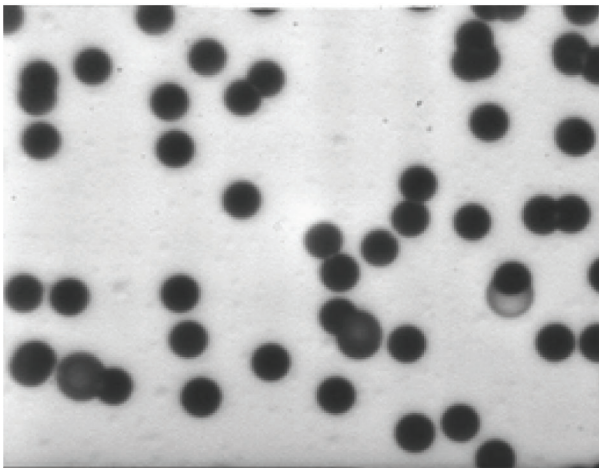


Figure 3: Digitalized etched tracks of alpha particles from collimated ^{210}Po -source. At the left side etched tracks as visible under light transmission microscope and right side shows track histogram with values of the distribution curve characteristics: mean value (19.81 mm), standard deviation (1.40 mm), skewness (16.25) and kurtosis (1501.47).

Particles detected by the 8pLP system are plotted in Figure 4. From the mentioned scattered plot we observe that protons, deuterons and tritons are in the low energy region (at the top of the diagram) followed by alphas along a curved region. Heavy ions cover the lower part of the displayed data having a lower value for pulse rising time, meanwhile,

partially scattered beam-like particles are in between the two regions.

Track-particle distribution given in Figure 5, corresponds to protons, deuterons, tritons and alphas; the beam-like charged particles (^7Li) and heavy masses are shown as a broad peak and distribution on the far right.

To obtain the number of particles for each group a deconvolution or unfolding model is devised. As a first approximation we consider a Gaussian distribution (as mentioned for the polonium alpha source) for all group of particles for which mean values and standard deviations are estimated a priori based on Figure 4.

4. Deconvolution of Complex Etched Nuclear Track Distribution

We explore the feasibility and difficulties during the unfolding of Gaussian spectres. For this, we assume that the measurement (y) is an accumulative stack of 5 Gaussian functions (describing the counts for protons, deuterium, tritium, alphas and heavy ions), that is

$$g(x, \mu, \sigma, \lambda) = \lambda \frac{e^{-\frac{(x-\mu)^2}{2\sigma^2}}}{2\sigma^2}, \text{ for } x \in, \quad (5)$$

$$y = G(x) = \sum_{i=1}^5 g(x, \mu_i, \sigma_i, \lambda_i) + \varepsilon, \varepsilon \sim N(\mu_\varepsilon, \sigma_\varepsilon),$$

where x is given, μ_ε and σ_ε are unknown but assumed constants. The variables μ , σ and λ are related to the means, standard deviations and amplitudes. There are 15 unknown parameters of the model, μ_i , λ_i and σ_i ($i = 1:5$). It is important to note that $\hat{\mu}_i (i = 1:5)$ are data and have a given precision for which μ_i approximates $\hat{\mu}_i$ taking into account the variability of these measurements. Given the physical nature of the problem, an additional restriction on the areas must be imposed.

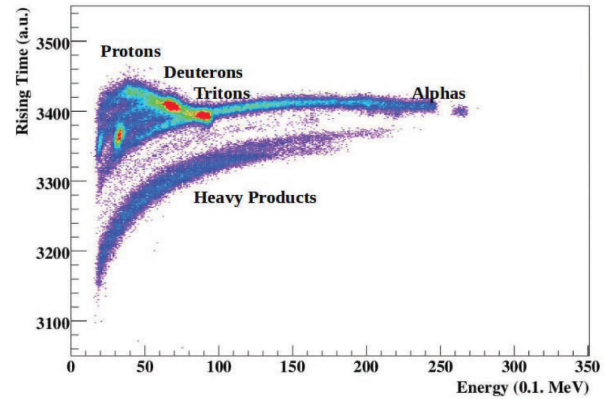


Figure 4: Scattered plot related to protons, deuterons and tritons. The alpha particles and heavy ions are shown as curved areas. The corresponding events given by the NTM is given in Figure 5. Fractions of area for each particle's spectre are:

$$f_1 = \frac{A_1}{A}, f_2 = \frac{A_2}{A}, f_3 = \frac{A_3}{A}, f_4 = \frac{A_4}{A}, f_5 = \frac{A_5}{A}, \quad (6)$$

where $\sum_{i=1}^5 A_i = A = \int y dx$.

The unknown areas A_i are approximated by $\int g_i(x) dx$.

To solve this problem using optimization, it is necessary to define an *objective* or *merit* function that takes into account

1. The approximation of the measurements (y) in the least-squares sense,

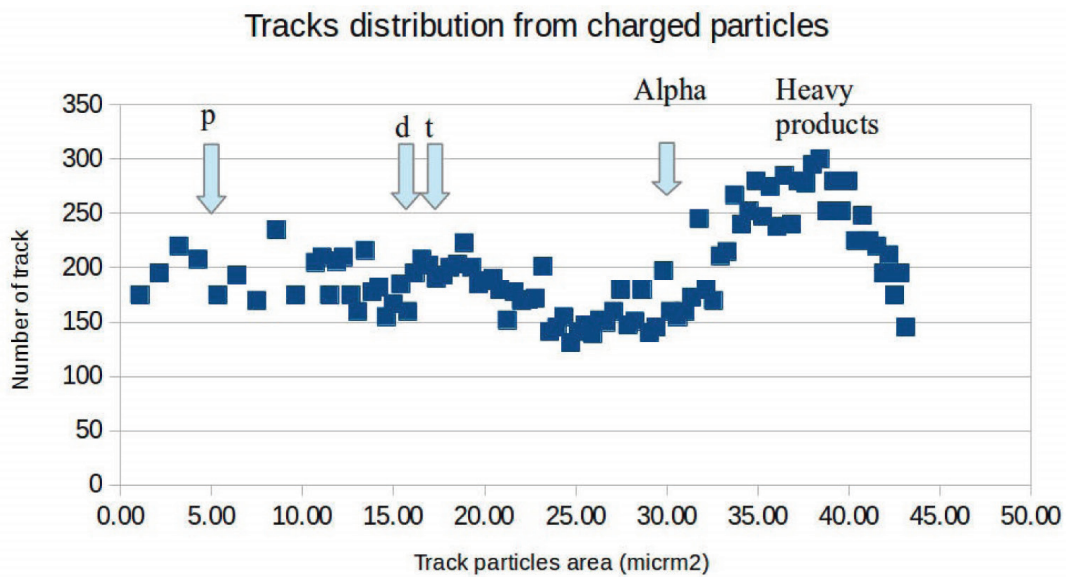


Figure 5: Track numbers associated to charged particle induced by reaction product and beam-like particles given in function of their area in mm^2 .

2. Approximates the fractions of the areas (A_i/A) to the available data (f_j), and
3. Allows some flexibility in the mean value parameters ($\hat{\mu}_j$).

Therefore, a possible merit function is

$$f(\mu, \sigma, \lambda) = \alpha \sum_j \left(\sum_{i=1}^5 g(x, \mu_i, \sigma_i, \lambda_i)_j - y_j \right)^2 + \beta \sum_{i=1}^5 \left(\frac{\int g(x, \mu_i, \sigma_i, \lambda_i) dx}{A} - f_i \right)^2 + \gamma \sum_{i=1}^5 (\mu_i - \hat{\mu}_i)^2, \quad (7)$$

where $\mu = (\mu_1, \dots, \mu_5)$, $\sigma = (\sigma_1, \dots, \sigma_5)$, and $\lambda = (\lambda_1, \dots, \lambda_5)$. The scalars α , β and γ are positive fixed parameters that require fine-tuning.

The problem to solve becomes

$$\begin{aligned} &\text{Minimize: } f(\mu, \sigma, \lambda) \\ &\text{subject to } \mu \in \mathbb{R}^5; \sigma, \lambda \in \mathbb{R}^5+. \end{aligned} \quad [10]$$

A significant issue with these problems is the selection of initial values. The merit function as defined has many local minima, and in order to obtain relevant solutions, *good* or *very good* initial guesses are required. It is also possible to bound the solution by imposing further restrictions on the standard deviation parameters (σ_j) and the scales (λ_j).

For this exercise, the problem was solved with the R statistical package [10] using the general-purpose optimization function, based on Nelder–Mead, quasi-Newton and conjugate-gradient algorithms. Fig. 6 shows a solution and Table 1 reports the optimal parameters values for the $f(\mu^*, \sigma^*, \lambda^*) = 3.642$, $\alpha = 10^{-4}$, $\beta = 1$ and $\gamma = 1$.

Table 1: Optimal values found for problem [6].

	Means (μ^*)	Std. Dev. (σ^*)	Scale (λ^*)	A_i/A (data)
Proton	3.04	2.77	1430	0.13 (0.08)
Deuterium	9.11	2.14	528	0.06 (0.07)
Tritium	11.6	3.52	614	0.07 (0.06)
Alpha	19.0	5.38	2433	0.29 (0.37)
Heavy Ions	37.1	6.49	4418	0.43 (0.42)

Some observations follow from the numerical experience. Once calibrated, the model can be used to unfold the accumulated counts. The results obtained encourage further experimentation in order to understand stability and generalization capacity. It is important to mention some

drawbacks of this approach. The many local minima make it difficult not only to fine-tune the model but also promotes the converging to undesirable solutions, for example, solutions with very large standard deviations. On the other hand, the problem is small enough to solve with other much more expensive alternatives such as optimization solutions coupled with some evolutionary strategy or even Bayesian approaches using Monte-Carlo Markov Chains. For the problem at hand, similar results were obtained when coupled to a marginal evolutionary strategy or solved using an Approximate Bayesian Computational method. Given the similarity in the obtained results, it is recommendable to solve using pure optimization methods, with equation 6. For applications where the discrimination of deuterium and tritium is not required a simpler model can be used where the mean, standard deviation and scale parameters are common for both elements, this not only reduces the problem dimensions but also simplifies the objective function.

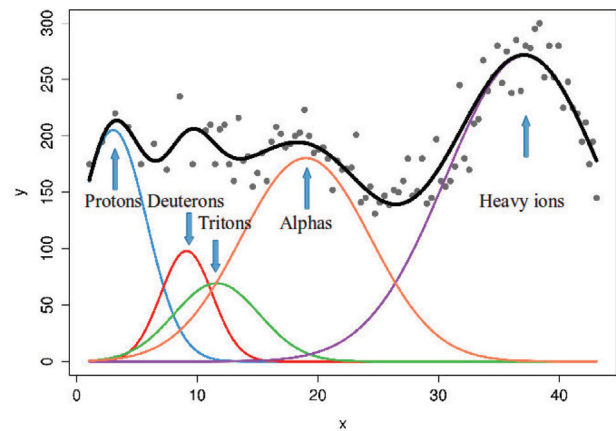


Figure 6: An optimal solution to problem [6] (black). Dots are counts in arbitrary unit (experimental data), and approximations: blue protons, red deuterium, green tritium, coral alpha and purple heavy ions in mass-channel number.

Conclusions

Passive detectors were exposed to reaction fragments to show that the NTM can be applied to study and detect trough induced damage, reaction products of light ions, alpha particles and 2–3AMeV energetic ions. Etched track histogram could be related through scattered plot assuming prior knowledge of particle tracks mean value and their standard deviation, so to apply a proper unfolding or deconvolution technique. Conveniently obtained data from previous experiment opens the possibility to correlate particle type (charge, mass and energy) and intensity of ${}^7\text{Li}+\text{Pb}$ at 31 MeV reaction products. From the applied unfolding method,

we may observe values for protons, which represent 8.3% of the total number of tracks; deuterons and tritons 12.3%, alpha particles frequency is 37.5% of recorded particle. Heavy ions and partially scattered beam-like particles are the most numerous with 41.8%. The main conclusion is that having sufficient experimental data (histogram of etched tracks), mathematical formalism exists to discriminate between groups of charged particles recorded by passive detectors giving valuable information on the reaction phenomenology. The most important information is that reaction products can be determined employing passive detectors when particle have low occurrence, different charge, mass and energy mass. This passive approach opens the possibility also for differential cross section measurements with the advantage an inexpensive detecting system. The drawback of the NTM is that results cannot be obtained on-line until the experiment is concluded.

Acknowledgements

One of the Authors (L. Sajo-Bohus) is grateful for the financial support given by Physics Institute of the University of Mexico (UNAM) while occupying the Cátedra Angel Dacal. Authors wish to thank the accelerator team of LNL-Legnaro-Italy for their technical skill, and to José-Ignacio Golzarri for his technical help. This work was performed under the partial economic support of UNAM-DGAPA-PAPIIT project IN-102819.

References

- [1] E. Fioretto, IEEE Transactions on Nuclear Science **44**, 1017 (1997). <https://doi.org/10.1109/23.603796>
- [2] J. K. Pálfalvi, L. Sajo-Bohus, Solid State Phenomena **238**, 16 (2015). <https://doi.org/10.4028/www.scientific.net/SSP.238.16>
- [3] M. Barbui, D. Fabris, S. Moretto, G. Nebbia, P. Nemeth, J.K. Palfalvi, S. Pesente, G. Prete, L. Sajo-Bohus and G. Viesti, Radiation Measurements **44**, 857 (2009). <https://doi.org/10.1016/j.radmeas.2009.10.048>
- [4] L. Sajo-Bohus, J.K. Pálfalvi, O. Arevalo, E.D. Greaves, P. Németh, D. Palacios, J. Szabo and I. Eördögh Radiation Measurements **40**, 442 (2005). <https://doi.org/10.1016/j.radmeas.2005.02.011>
- [5] B. Dörschel, D. Hermsdorf and K. Kadner, Radiation Measurements **35**, 183 (2002). [https://doi.org/10.1016/S1350-4487\(02\)00049-5](https://doi.org/10.1016/S1350-4487(02)00049-5)
- [6] J.K. Palfalvi, L. Sajo-Bohus and S. A. Durrani, Radiation Protection Symposium Obergurl/Tyrol 28-30- April, Proceedings **2**, 271 (1993).
- [7] N. Rozlosnik, L. Sajo-Bohus, C. Birattari, E. Gadioli, L.P. Biró and K. Havancsák, Nanotechnology **8**, 32 (1997). <https://doi.org/10.1088/0957-4484/8/1/008>
- [8] Z. Lounis, S. Djefal, K. Morsli, M. Alla, Nucl. Instr. Meth. Phys. Res. B **179**, 543 (2001). [https://doi.org/10.1016/S0168-583X\(01\)00601-2](https://doi.org/10.1016/S0168-583X(01)00601-2)
- [9] W. Gonzalez et al., Journal of Nuclear Physics, Material Sciences, Radiation and Applications **2**, 83 (2014). <https://doi.org/10.15415/jnp.2014.21006>
- [10] R Development Core Team, 2015. R: A language and environment for statistical computing. R Foundation for Statistical Computing, Vienna, Austria. ISBN 3-900051-07-0, URL. <http://www.R-project.org>. Accessed August 28, 2019.



Journal of Nuclear Physics, Material Sciences, Radiation and Applications

Chitkara University, Saraswati Kendra, SCO 160-161, Sector 9-C,
Chandigarh, 160009, India

Volume 7, Issue 2

February 2020

ISSN 2321-8649

Copyright: [© 2020 G. Espinosa et al.] This is an Open Access article published in Journal of Nuclear Physics, Material Sciences, Radiation and Applications (J. Nucl. Phys. Mat. Sci. Rad. A.) by Chitkara University Publications. It is published with a Creative Commons Attribution- CC-BY 4.0 International License. This license permits unrestricted use, distribution, and reproduction in any medium, provided the original author and source are credited.
